stream-transpiration cooling problem," J. Aerospace Sci. 28, 449–456 (1961).

[13] Howe, J. T., "Some finite difference solutions of the laminar compressible boundary layer showing the effects of upstream transpiration cooling," NACA Memo. 2-26-59A (1959).

[14] Rubesin, M. W., Pappas, C. C., and Okuno, A. F., "The effect of fluid injection on the compressible turbulent boundary layer–preliminary tests on transpiration cooling of a flat plate at $M = 2.7$ with air as the injected gas," NACA RM A55119 (December 1955).

JUNE 1966 AIAA JOURNAL VOL. 4, NO. 6

Observations of Turbulent Reattachment behind an Axisymmetric Downstream-Facing Step in Supersonic Flow

ANATOL ROSHKO* AND GERALD J. THOMKE†
Douglas Aircraft Company Inc., Santa Monica, Calif.

Supersonic flow over a downstream-facing step on the circumference of a large, ducted, axisymmetric body was used to study flow reattachment. Step heights h were 0.25, 1.00, and 1.68 in., compared to a body radius of 6 in. Freestream Mach numbers were in the range 2 to 4.5. The turbulent boundary-layer thickness just ahead of the step varied from 0.14 to 0.19 in. (momentum thicknesses of about 0.01 in.).

Surface pressure distributions throughout the region of separation and reattachment were measured, and points of reattachment were determined. Comparison of the shapes of the pressure distributions for various step heights shows that the initial (steepest) parts of the reattachment pressure rise, up to the point of reattachment, tend to become superimposed when plotted against x/h. Downstream of reattachment the curves branch out, exhibiting a dependence on geometry and probably on initial shear layer profile. In the region of the initial pressure rise (near the end of the "dead air" region) dynamic pressures are low; the pressure rise there apparently is balanced by turbulent shear stress.

Nomenclature

h = step height
M_e = Mach number of the base flow external to the free shear layer
M_s = Mach number of the external flow just upstream of the separation point
M_∞ = Mach number of the freestream
od = location of flow reversal point determined from the orifice dam technique
p = local surface pressure
p' = local surface pressure in the presence of an orifice dam
p_b = static pressure in the base (dead air) region
p_e = static pressure of the flow external to the free shear layer, $= p_b$
p_s = surface pressure just upstream of the separation point
p_∞ = static pressure of the freestream
pp = location of the peak in surface pressure distributions measured in the presence of orifice dams
r = reattachment or flow reversal point
Re_∞' = test section freestream unit Reynolds number
R_s = radius of the model forebody at the flow separation point
s = separation point
sf = location of flow reversal point from the surface flow technique
u = local velocity in the boundary layer
u_e = velocity just outside the boundary layer and ahead of the step
x = distance along the model measured downstream from the base of the step
y = height measured from the surface of the model outward into the air-stream
δ_s = boundary-layer thickness just ahead of the step
δ_s^* = boundary-layer displacement thickness just ahead of the step
θ_s = boundary-layer momentum thickness justa head of the step

Received May 17, 1965; revision received March 17, 1966. This study was sponsored by the Douglas Aircraft Company Independent Research and Development Program, Account 80301-016. The authors are indebted to many staff members of the Douglas Aerophysics Laboratory, El Segundo, California, who contributed to the experimental program. Particular thanks go to W. E. Smith for his extensive help in preparing the experiment and report, and for many helpful discussions.

* Consultant; also Professor of Aeronautics, Graduate Aeronautical Laboratories, California Institute of Technology. Associate Fellow Member AIAA.

† Engineer-Scientist, Aerophysics Laboratory. Associate Member AIAA.

Introduction

THE importance of the reattachment region in problems of flow separation is well-known. The flow configuration in which it has been studied most frequently is the flow over a base, or downstream-facing step. Although this appears, at first, to be a very simple configuration for experimental and theoretical attack, at present there is considerable uncertainty and controversy about it, both experimentally and theoretically.

On the experimental side, the long standing effort to define a base pressure vs Mach number curve, so far, has not resulted in a definitive result. Reynolds number effects, often interpreted in terms of boundary-layer thickness at the separation point, have been especially difficult to clarify. This is due to several factors: lack of appreciation, at first, for the need to establish clearly the boundary-layer conditions; lack of appreciation of the importance of geometrical configuration for correlating various results; difficulties of avoiding a turbulent-transitional condition in the ordinary range of laboratory facilities; and, sometimes, difficulties with end effects on two-dimensional models.

On the theoretical side, the well known Korst-Chapman reattachment criterion[1,2] recently has been the subject of critical re-examination; various experimental examples[3,4] of

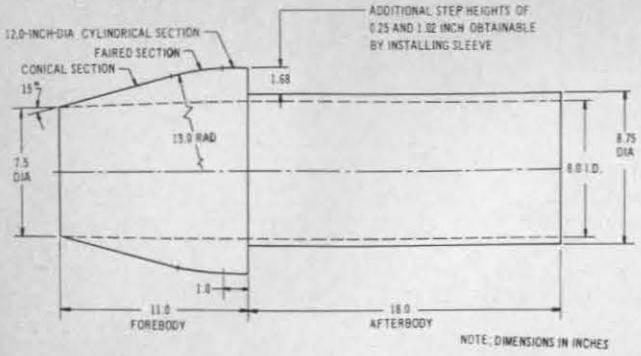

Fig. 1 Axisymmetric ducted model.

reattachment pressure rise greater than the maximum given by the criterion have redirected attention to a basic inconsistency in that theory and to attempts at modifying it.[3,5] In another approach, the earlier, partially successful integral methods such as that of Crocco and Lees[6] are being improved.[7,8]

The present paper describes some experiments on turbulent flow over a downstream-facing step. These provide some insights into the reattachment problem and constitute a set of pressure distributions against which theoretical results can be tested. The experiments were motivated largely by the availability of a large facility with high unit Reynolds number: the Four-Foot Trisonic Wind Tunnel at the Douglas Aerophysics Laboratory. In this it was possible to use the large axisymmetric model shown in Fig. 1 and still avoid the problem of wake interference from wave reflections off the side walls. Other advantages were the following: with the axial symmetry, problems of end effects were eliminated; and with the large size, step heights could be small relative to body radius, but still reasonably large compared to boundary-layer thickness. The latter effect was enhanced by using a ducted model, which made it possible to have a much shorter length from nose to step than with the usual cone-cylinder body. The length was still sufficient to insure transition well ahead of the step. In this way we hoped to eliminate end-wall effects and transition effects, while keeping the boundary-layer thickness at separation small compared to step height. On the other hand, the axial symmetry introduces a geometrical parameter that varies with step height.

Experimental Conditions‡

The model (Fig. 1) had a diameter of 12 in. at the separation shoulder, with a 1.68-in. step down to the cylindrical afterbody. The step height could be changed to 1.00 or 0.25 in. by installation of sleeves over the afterbody. Measurements were made over the range of freestream Mach numbers from 2.0 to 4.5 at the values listed in Table 1, in which other pertinent conditions are listed. The reference conditions (M_s, p_s) just ahead of the step are somewhat different from freestream values. This is due to the flowfield of the forebody. It would have been preferable to use a straight cylinder for the outer surface of this forebody, and thus to have a uniform flowfield ahead of the step, with $M_s = M_\infty$, etc.; but this would have required the inner surface (the duct) to be convergent, resulting in choking at the lower Mach numbers.

Transition, observed on shadowgraphs, occurred in all cases near the end of the conical section of the forebody. The boundary-layer thicknesses just ahead of the step (Table 1) were determined from velocity profiles (Fig. 2) obtained by conventional pitot-tube surveys, using a constant-energy assumption (in all cases the model surface temperature was within 2% of the freestream total temperature). The profiles shown in Fig. 2 were obtained at x_s, the streamwise position of the shoulder; the probe just cleared the edge in order to traverse past it. A few profiles taken 0.25 in. ahead of the shoulder were identical with those in Fig. 2, except for points at values of $y/\delta_s < 0.1$; the flow in these lower layers evidently is influenced by the expansion over the shoulder. In the calculations of δ^* and θ, those points were ignored and the profiles were faired smoothly into the origin. The corresponding shape factors δ^*/θ, agree closely with calculations based on the theory in Ref. 10.

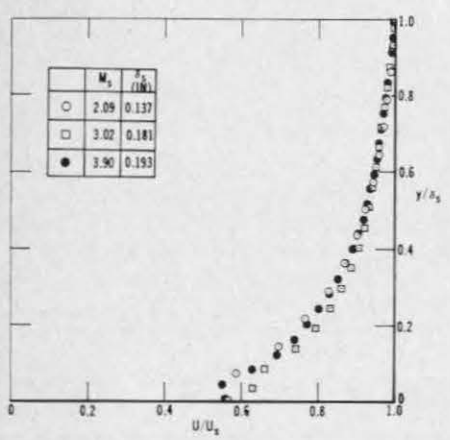

Fig. 2 Boundary-layer velocity profiles at step shoulder.

‡ A detailed description of the experimental set up and results is given in Ref. 9.

Measurements

An example of a flowfield downstream of the step is shown in the schlieren picture of Fig. 3 taken at $M_s = 2.09$. Sketched on the picture is a broken line indicating the theoretical position of the free streamline in the corresponding inviscid

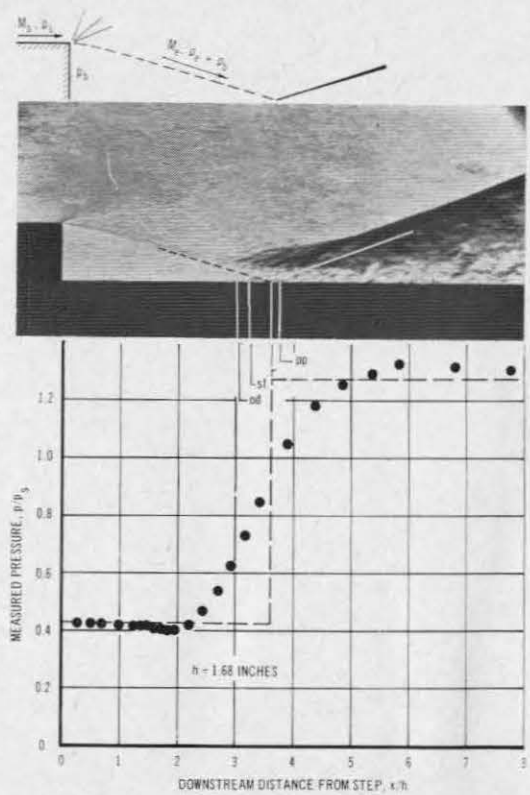

Fig. 3 Typical flowfield at $M_s = 2.09$, with corresponding pressure distribution.

Table 1 Summary of Experimental Parameters[a]

M_∞	M_s	p_s/p_∞	Re_∞' (10^6/in.)	h (in.)	δ_s/h	δ_s^*/h	θ_s/h	p_b/p_s	M_e	Reattachment Region $(x/h)_r$	$(x/h)_{pp}$	$(x/h)_{sf}$	Parameters $(x/h)_{od}$
2.008	2.09	0.81	0.95	0.250	0.5480	0.1368	0.0389	0.373	2.72	3.36	...	3.80	...
(2.0)				1.020	0.1343	0.0335	0.0095	0.392	2.69	3.73	3.70	3.34	3.00
				1.675	0.0818	0.0204	0.0058	0.417	2.65	3.60	3.75	3.25	3.45
2.497	2.56	0.81	1.02	0.250	0.6560	0.1791	0.0415	0.274	3.42	3.02	...	2.90	...
(2.5)				1.675	0.0979	0.0267	0.0062	0.331	3.29	3.35	...	3.13	...
2.996	3.02	0.83	1.36	0.250	0.7240	0.2211	0.0402	0.214	4.12	2.88	...	2.32	...
(3.0)				1.020	0.1774	0.0542	0.0099	0.198	4.17	3.02	2.90	2.65	2.50
				1.675	0.1081	0.0330	0.0060	0.252	3.99	3.24	3.30	3.10	2.70
3.489	3.49	0.84	1.43	0.250	0.7600	0.2614	0.0382	0.184	4.78	2.98	...	2.20	...
(3.5)				1.675	0.1134	0.0390	0.0057	0.174	4.83	3.06	...	2.47	...
3.975	3.90	0.86	1.30	0.250	0.7720	0.3049	0.0359	0.194	5.23	3.46	...	2.30	...
(4.0)				1.020	0.1892	0.0747	0.0088	0.132	5.57	3.12	...	2.00	...
				1.675	0.1152	0.0455	0.0054	0.122	5.65	2.97	...	...	2.40
4.460	4.37	0.87	1.20	1.675	0.1170	0.0529	0.0052	0.111	6.34	3.19	...	...	...
(4.5)													

[a] Note: Boundary-layer parameters at $M_\infty = 2.5$, 3.5, and 4.5 obtained by interpolating and extrapolating data measured at $M_\infty = 2$, 3, and 4.

model, computed§ for the measured value of base pressure, $p_b = 0.424\ p_s$. Taking $p_e = p_b$ to be the pressure in the external flow at the edge of the shear layer, which is assumed to have expanded isentropically from p_s, gives the corresponding $M_e = 2.64$. If continued to the shoulder, this line coincides with the shear layer visible on the photograph. Also sketched is a line indicating the theoretical position of an oblique shock wave originating at r in the inviscid model. It may be compared, in the photograph, to the dark recompression region beginning somewhat upstream of r. Also shown is the measured pressure distribution along the surface and, for comparison, the pressure jump at r in the inviscid model. (The other notation on the figure is explained later.)

Figure 4 is a plot of the pressure distributions measured along the surface downstream of the step at three Mach numbers for three different step heights. The broken lines (Fig. 4) are the basic pressure distributions (for zero step height) due to the nose shape (cf. previous remarks) computed by the method of characteristics.¶ The measured pressure distributions for the various step heights all tend toward this basic distribution far downstream. For the larger step heights, the pressure in the reattachment region overshoots the basic distribution, due to an axisymmetric effect in the equivalent free streamline flow.[12] The effect diminishes with decreasing h/R_s or with increasing Mach number; i.e., smaller step height or higher Mach number tends to make the flow in the vicinity of the step more nearly two-dimensional. Thus, in Fig. 4, for the smallest step ($h = 0.25$ in.), the pressure rises monotonically and fairs into the basic pressure distribution without overshoot. Also, with increasing Mach number, the larger steps show less overshoot.¶ Measurements of circumferential pressure distribution gave values that were uniform within 0.5% in the base region and within 2% in the region of rising pressure.

In Fig. 4 it is difficult to see the details of the pressure distributions in the so-called dead-air region near the step face; these are shown in Fig. 5, in which the pressures over the step face (represented as $-1 < x/h < 0$) and several step heights downstream are plotted. The values selected for the base pressures are indicated by broken lines. It may be seen that these are biased toward the values on the step face, and that there is a characteristic small dip in pressure just before the reattachment pressure rise begins. For each value of base pressure p_b ($= p_e$), the corresponding value of M_e (Fig. 3) was computed by assuming an isentropic expansion from (M_s, p_s). These values are listed in Table 1. We are not including here plots of base pressure against Mach number; these can, however, readily be determined from the information in Table 1, in which data for boundary-layer correlations also may be found.

Point of Reattachment

Two techniques were used to locate the point of reattachment. One of these was a surface flow technique using a coating of titanium dioxide (TiO_2) in oil. Figure 6 shows an example of the flow pattern at $M_\infty = 3$ for the large step, $h = 1.68$ in. The line of flow reversal is quite well defined.** The positions of flow reversal points located in this way are indicated by *sf* in Figs. 3 and 4 and are listed in Table 1. In the second technique, small obstructions (0.05 in. high and 0.15 in. wide), which we call orifice dams, were cemented just upstream of each of the orifices along the surface (Fig. 7). Each such orifice and dam is a rough approximation to a sur-

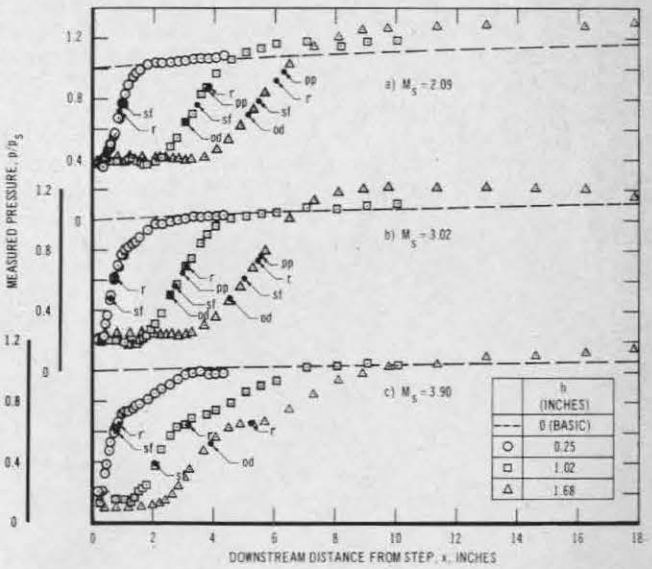

Fig. 4 Measured pressure distributions.

§ We made use of the free streamline calculations in Ref. 11.

¶ We are indebted to J. Xerikos, of the Douglas Aircraft Company, for providing us with these results, which are described more fully in Ref. 9.

** Also evident is a three-dimensional pattern that is similar to that observed by Ginoux[13] in laminar two-dimensional flow over a step, and which is indicative of secondary motions in the reattachment region. Their effect on the reattaching flow is unknown. Some detailed pressure distributions in that region indicate that these secondary motions have very small effect on the static pressure distribution, and it seems unlikely that the over-all pressure rise is affected.

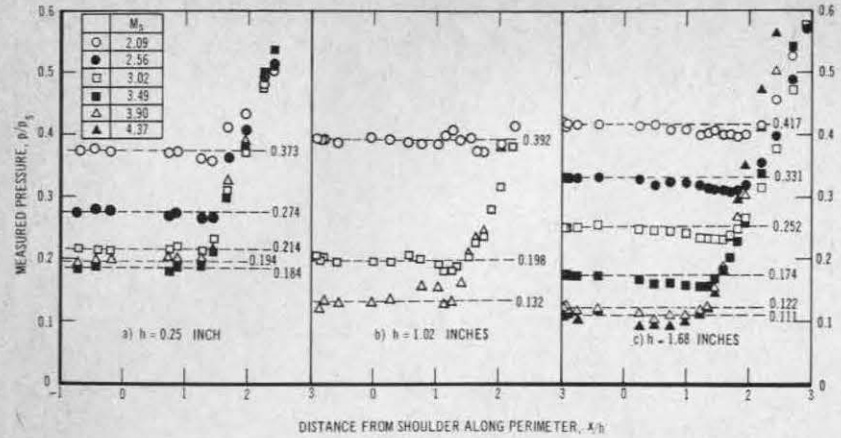

Fig. 5 Measured pressure distributions along the perimeter of the base region. Broken lines indicate values used for p_b/p_s. Step face is represented by negative values of x/h.

face pitot (Preston) tube; in forward flow it should show a decrease of pressure, compared to the clear surface, since the orifice is on the "base" side of the dam; whereas in reverse flow it should show an increase, the orifice now being on the "face" side. Thus, the streamwise pressure distributions with and without orifice dams should cross at the point of flow reversal.

An example of the results obtained is shown in Fig. 7. It may be seen that the effect is very small, an indication of the low dynamic pressures in the reverse flow region up to the reattachment point. A plot (not shown) of the ratio of the two pressures p and p' (the crossover point being at $p'/p = 1$) improved the resolution considerably. The result was quite unambiguous for the lowest Mach number, 2.09, but rather less accurate for the other two, due to scatter. The method was not applied to the smallest (0.25 in.) step. Locations of flow reversal points determined in this way are indicated by *od* in Figs. 3 and 4 and are listed in Table 1.

An unexpected result from the orifice dam technique was the appearance of a peak in the pressure distribution, as in Fig. 7. The decrease in pressure after the peak, even though the general static pressure is still rising, indicates that the flow over the dam has become strong enough to produce an appreciable dynamic effect and a strong decrease of the base pressure on the dam. Thus, the peak is a good indication of the end of the (nearly) dead-air region. The locations of these peak pressure points are indicated by *pp* in Figs. 3 and 4 and are listed in Table 1. It may be seen that they always lie close to the points marked *r*, which are the theoretical locations of the reattachment points in the corresponding inviscid free streamline model (Fig. 3). On the other hand, the points of flow reversal, whether *sf* or *od*, always occur at smaller values of x/h. (The one exception, for the smallest step at $M_s = 2.09$, may be in error; the corresponding flow pattern was not distinct.) Taken together, these results suggest that the real point of "reattachment" (better called the point of flow reversal) lies just inside the region of low dynamic pressure, which itself corresponds fairly well to the so-called dead-air region of the free streamline model.

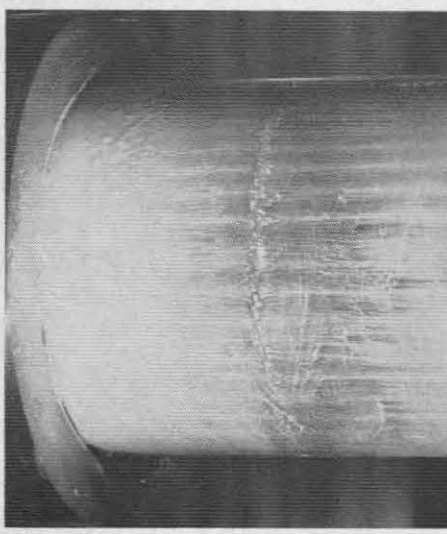

Fig. 6 Reattachment flow pattern obtained using oil-flow visualization technique; $M_s = 3.02$, $h = 1.68$ in.

Shape and Scale of Pressure Distributions

To study the shapes of the pressure distributions of Fig. 4, the curves were replotted against the dimensionless distance x/h. In Fig. 8 the distributions are arranged in groups of constant Mach number, to bring out the effects of geometry, whereas in Fig. 9 they are arranged in groups of constant h, to display the Mach number effect for given geometry.

Due to the crowding together of these curves, the locations of the points *sf*, *r*, and *pp* from Fig. 4 are not reproduced in Figs. 8 and 9, but their ranges are indicated in Fig. 8. An interesting trend is that the location of *r* (or *pp*) tends to remain nearly fixed (at a value of x/h slightly greater than 3), but the location of *sf* tends to move toward the step with increasing Mach number. This should be viewed with some reservation, since results from surface flow techniques are notoriously difficult to evaluate; on the other hand, there is indication of the same trend in *od* from the orifice dam experiments.

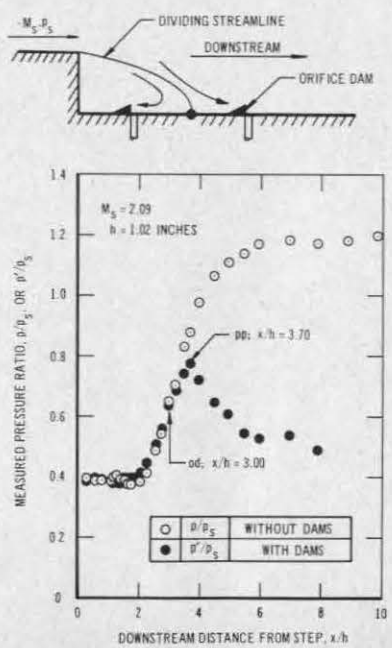

Fig. 7 Effect of orifice dams on pressure distribution.

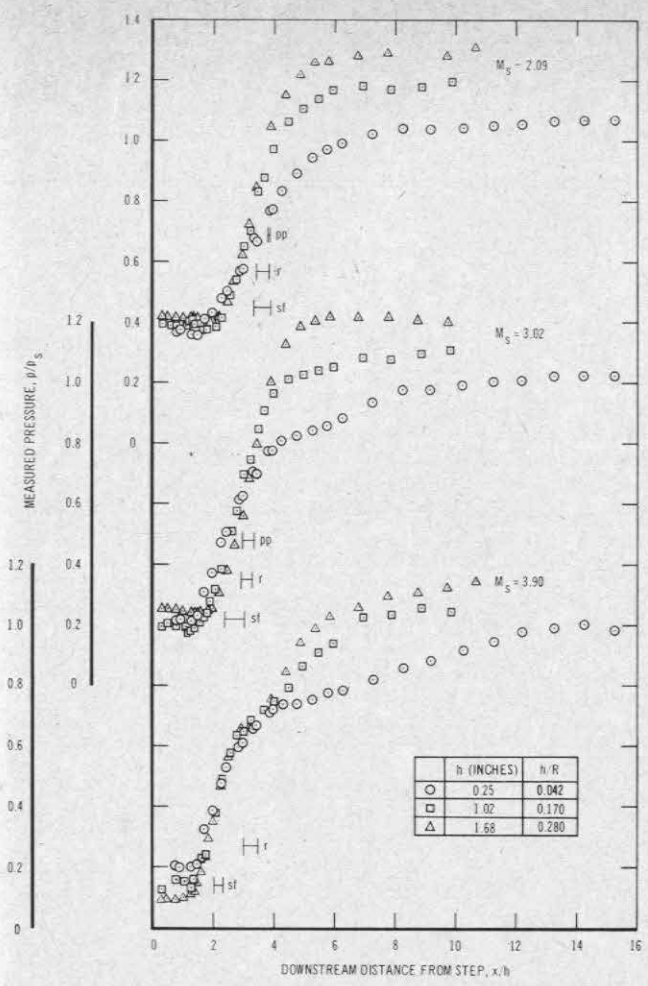

Fig. 8 Effect of step height on shapes of measured pressure distributions; ranges of *pp*, *r*, and *sf* noted.

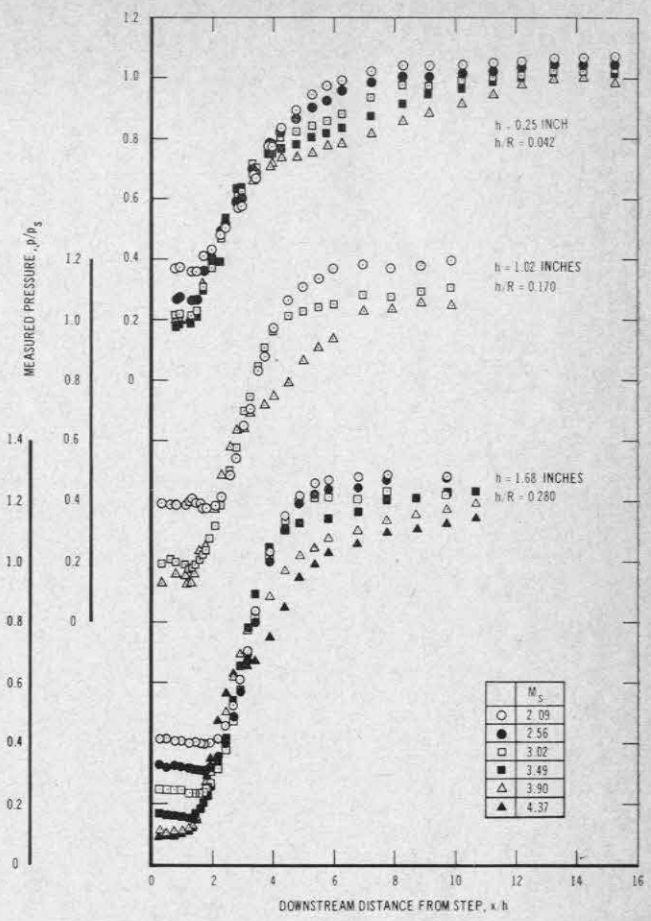

Fig. 9 Effect of Mach number on shapes of measured pressure distributions.

In Fig. 9, the effects of Mach number are compared for fixed geometries. The group for the smallest step height (0.25 in.) is particularly interesting since it includes five different values of Mach number and since $h/R_s = 0.04$ is small enough that the reattaching flow surely can be regarded as two-dimensional. A noteworthy feature is the branching of the curves just downstream of the reattachment point; a break in the pressure distribution there becomes more pronounced with increasing Mach number. The same trend is evident for the other two values of h.

Figures 8 and 9 are remarkable in the tendency shown for the pressure distributions to be superimposed on each other in the region of steepest pressure rise, approximately $2 < x/h < 4$. One might expect the length scale of the pressure rise to depend on the thickness to which the shear layer has grown before it reattaches, and the scaling with h seems to imply that the initial thickness is small enough to be unimportant for the length scale of the reattachment region (not necessarily for the dynamics). On the other hand, the initial thickness δ_s for our smallest step height is comparable to h (Table 1); furthermore, some measurements by Hastings[14] included cases in which δ_s was considerably larger than h, and still the pressure rise region tended to superimpose on those for smaller δ_s/h; the base pressures, however, were affected considerably. All this suggests that the dead-air or inner portion of the flow is governed largely by developments along the dividing streamline, i.e., that an inner shear layer, beginning at the separation point and growing linearly, will be consistent with a scaling that depends mainly on step height

It has been remarked earlier that, up to the reattachment point, dynamic pressures seem to play a small role, and the pressure rise in this region must be balanced mainly by turbulent shear stress. The breaks in the pressure distribution just downstream of reattachment and, in particular, the bump at $x/h = 3$ for $M_s = 4.37$, (Fig. 9), may be related to the lip shock phenomena discussed by Weinbaum[15] and observed by Hama.[16]

Finally, as noted earlier, the superposition of the pressure distributions up to reattachment contrast with the variety of developments further downstream, suggesting an independence from the flow downstream of reattachment; this independence has been observed more explicitly in experiments by Bogdonoff et al.[17] and Carrière and Sirieix,[4] as well as in the theoretical results of Crocco-Lees-Reeves,[6,8] where it is attributed to the appearance of a critical condition just after reattachment. The peak pressure observed in the orifice dam experiments (described previously) also occurs at this point, suggesting a large and sudden acceleration of the boundary layer there.

References

[1] Korst, H. H., "A theory for base pressures in transonic and supersonic flow," J. Appl. Mech. **23,** 593–600 (1956); also Korst H. H., "Comments on the effect of boundary layer on sonic flow through an abrupt cross-sectional area change," J. Aeronaut. Sci. **21,** 568 (1954); also Korst, H. H., Page, R. H., and Childs, M. E., "A theory for base pressures in transonic and supersonic flow," Univ. of Illinois ME-TN-392-2, Office of Scientific Research, TN 55-89 (March 1955).

[2] Chapman, D. R., Kuehn, D. M., and Larson, H. K., "Investigation of separated flows in supersonic and subsonic streams with emphasis on the effect of transition," NACA Ames Research Lab. Rept. 1356 (1958); also, NACA Ames Research Lab. RM A55L14 (June 1956).

[3] Nash, J. F., "An analysis of two-dimensional base flow including the effect of the approaching boundary layer," Aeronautical Research Council R&M 3344 (1963).

[4] Carrière, P. and Sirieix, M., "Résultats récents dans l'étude des problèmes de mélange et de recollement," 11th International Congress of Applied Mechanics Munich (August–September 1964); also Office National D'Études et de Recherches Aérospatiales, Tiré a Part 165 (1964).

[5] McDonald, H., "Turbulent shear layer reattachment with special emphasis on the base pressure problem," Aeronaut. Quart. **15**, 247–280 (August 1964).

[6] Crocco, L. and Lees, L., "A mixing theory for the interaction between dissipative flows and nearly isentropic streams," J. Aerospace Sci. **19**, 649–676 (1952).

[7] Lees, L. and Reeves, B. L., "Supersonic separated and reattaching laminar flows," AIAA J. **2**, 1907–1920 (1964).

[8] Reeves, B. L. and Lees, L., "Theory of laminar near wake of blunt bodies in hypersonic flow," AIAA J. **3**, 2061–2074 (1965).

[9] Thomke, G. J., "Separation and reattachment of supersonic turbulent boundary layer behind downstream facing steps and over cavities," Douglas Aircraft Co. Rept. SM 43062 (March 1964).

[10] Reshotko, E. and Tucker, M., "Approximate calculation of the compressible turbulent boundary layer with heat transfer and arbitrary pressure gradient," NACA Lewis Research Center TN 4154 (1957).

[11] Sims, J. L., "Results of the computations of supersonic flow fields aft of circular cylindrical bodies of revolution by the method of characteristics," Army Ballistic Missile Agency Rept. DA-R-49 (March 1958).

[12] Chapman, D. R., "An analysis of base pressure at supersonic velocities and comparison with experiment," NACA Ames Aeronautical Lab. Rept. 1051 (1951).

[13] Ginoux, J., "Experimental evidence of three-dimensional perturbations in the reattachment of a two-dimensional laminar boundary layer at $M = 2.05$," Training Center for Experimental Aerodynamics, Belgium, TN-1 (1958).

[14] Hastings, R. C., "Turbulent flow past two-dimensional bases in supersonic streams," Royal Aircraft Establishment TN Aero. 2931 (AD 433011) (December 1963).

[15] Weinbaum, S., "The rapid expansion of a supersonic shear flow," Avco-Everett Research Lab., Research Rept. 204 (1965).

[16] Hama, F. R., "Estimation of the strength of the lip shock," AIAA J. **4**, 166–167 (1966).

[17] Bogdonoff, S. M., Kepler, C. E., and Sanlorenzo, E., "A study of shock wave turbulent boundary layer interaction at $M = 3$," Princeton Univ. Aeronautical Engineering Dept., Rept. 222 (1953).